Electronic Supplementary Material (ESI) for Chemical Communications

Supporting Information

Synthesis of Superior Fast Charging/Discharging Nano-$LiFePO_4$/C from Nano-$FePO_4$ Generated with a Confined Area Impinging Jet Reactor Approach

Xiao-min Liu[‡, a], Pen Yan[‡, a], Yin-Yin Xie[b], Hui Yang*[,a], Xiao-dong Shen [a], and Zi-Feng Ma[b,c]

[a] College of Materials Science and Engineering, Nanjing University of Technology, 5 Xinmofan Road, Nanjing, Jiangsu, 210009, China. Tel: +86-25-83587275; E-mail: yanghui@njut.edu.cn

[b] Sinopoly Research Center, Sinopoly Battery Limited, Shanghai, 200240, China

[c] Institute of Electrochemical and Energy Technology Department of Chemical Engineering, Shanghai Jiao Tong University, Shanghai, 200240, China

[‡]They contribute equally to this work.

Experimental Section

Synthesis of $FePO_4$: Solution A (0.3 mol·L^{-1} $Fe(NO_3)_3$) and solution B (0.3 molL^{-1} $(NH_4)_2HPO_4$) were prepared by dissolving $Fe(NO_3)_3 \cdot 9H_2O$ (AR, Aldrich) and $(NH_4)_2HPO_4$ (AR, Aldrich) in deionized water, respectively. The two reaction solutions were simultaneously injected into an impinging jet reactor with the same volume speed, 100 mL·min^{-1}, by a two-channel precision syringe pump (PHD2000, Harvard Apparatus, USA). The white $FePO_4 \cdot xH_2O$ precipitates were generated immediately and collected by centrifuge. The products were washed with deionized water for several times, and then dried in a vacuum oven overnight before further processing.

Preparation of $LiFePO_4$/C composite: $LiOH \cdot H_2O$ (AR, Aldrich), trigonal $FePO_4$ and glucose (AR, Aldrich) with the molar ratio of 1.02:1:0.183 were well mixed by ball-milling for 6h. The resulting mixture was first preheated at 350 ℃ for 6h, then calcined at 700 ℃ for 10h under an Ar/H_2 (93 Vol%/7Vol%) atmosphere to produce the $LiFePO_4$/C composite.

Characterization of $FePO_4$ and $LiFePO_4$/C composite: The crystal structure of the synthesized $FePO_4$ and $LiFePO_4$/C was characterized by X-ray powder diffraction (XRD, D/MAX-2500VL/PC, Rigaku, Japan). The diffraction data were collected for 4.8s at each 0.02^o step width from 10 to 70^o. The thermal decomposition behavior was examined by thermogravimetry-differential scanning calorimetry (TG-DSC) in the temperature range of 25–900 ℃ at the heating rate of 10 $℃ \cdot min^{-1}$ under nitrogen atmosphere. The morphology was observed using a JSM−6700F field emission scanning electron microscope (FESEM) and a Joel JEM−1010 transmission electron microscope (TEM). The content of the in-situ carbon-coating was determined by the carbon/sulphur analyzer (HCS-040G, DEKAI INSTRUMENTS, China). The ion ratio was determined by inductively coupled plasma-atomic emission sepctrometry (ICP, Iris Advantage 1000, Thermo Electron Corporation, USA)

Electrochemical measurements: The electrochemical performance was characterized by 2032 cell coins assembled in an argon-filled glove box. A slurry was made by dispersing the active material $LiFePO_4$/C, super-p carbon black and polyvinylidene fluoride homogeneously at the weight ratio of 75:15:10 in N-methyl-pyrolidinone. Then the mixed slurry was coated uniformly onto an aluminium foil, followed by drying in a vacuum oven at 120 ℃ for 10 h. The foil was punched to electrode disks in a diameter of 13 mm. The electrodes were pressed, dried and weighed to determine the active mass. A typical electrode disk contained ~ 4.2 $mgcm^{-2}$ of the $LiFePO_4$/C composite. The 2032 coin cell was assembled using Celgard 2400 as the separator, lithium foil as the counter electrode, and 1 $molL^{-1}$ $LiPF_6$ (EC: DEC=1:1 in Vol) as electrolyte. The cells were tested at different rates in the voltage range of 2.0V and 4.3V at room temperature using a BT-2000 battery testing system (Arbin, USA).

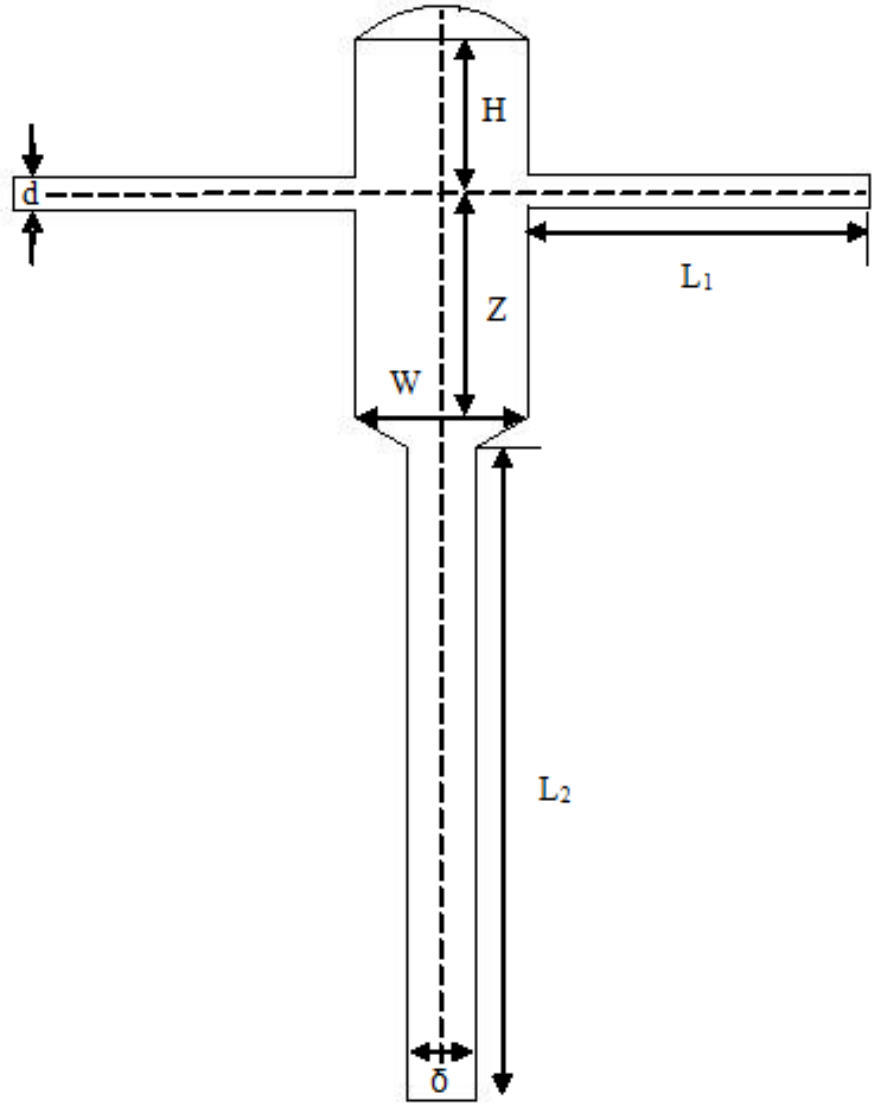

Figure s1. The schedamatic diagram of the confined area impinging jet reactor

(d=1mm; δ=2d; W=4.76d; H=0.8W; Z=1.2W; L1=10d; L2=10δ)

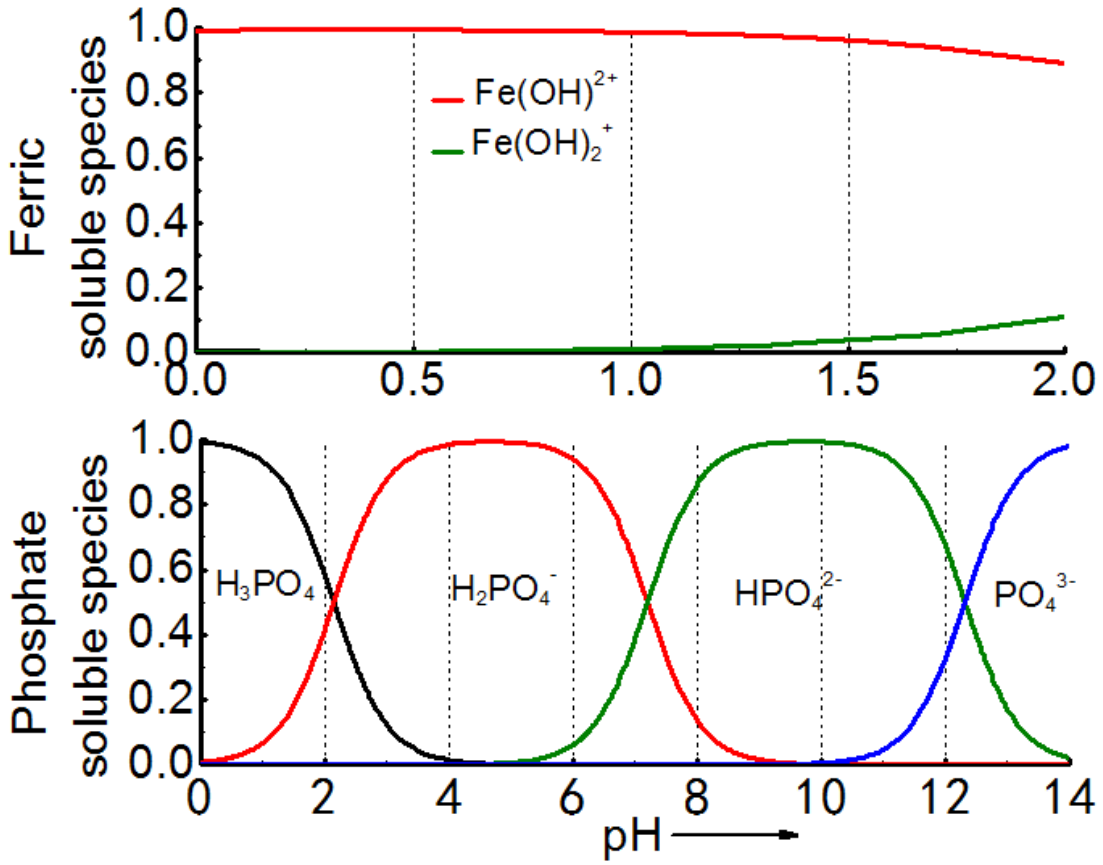

Figure s2. The hydrolysis of ferric (up) and phosphate (down) at various pH values

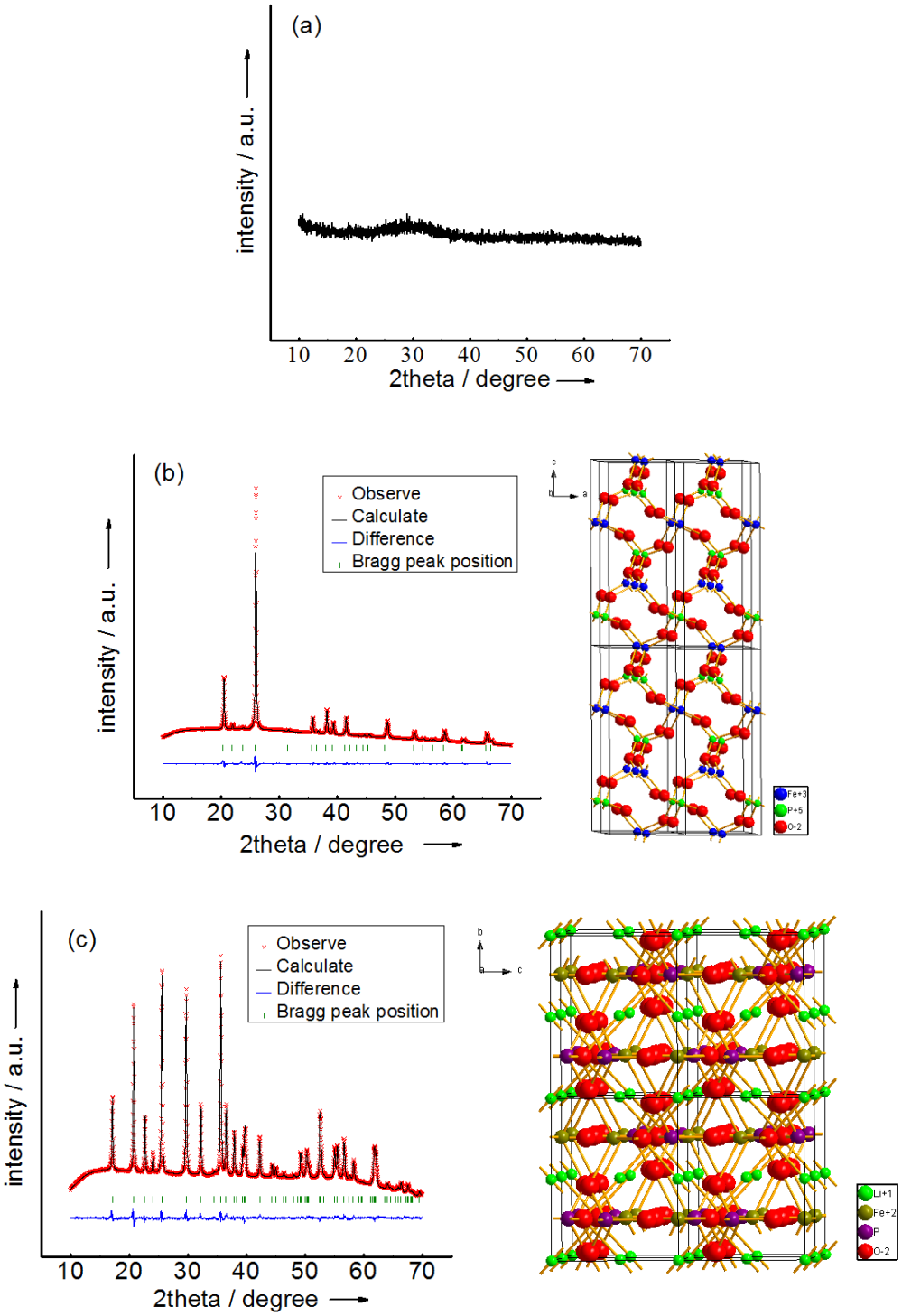

Figure s3. (a) XRD patterns of the precipitate $FePO_4$; Rietveld refinement of XRD patterns and the corresponding crystal structure of (b) the $FePO_4$ after heat treatment at 600 ℃ for 10 hours and (c) the $LiFePO_4$/C.

Table s1. Rietveld refinement results of XRD patterns of the $FePO_4$ and $LiFePO_4$/C

Formula		$FePO_4$		
Crystal system		*Trigonal*		
Space group		P3121		
Atom	x	y	z	g
Fe	0.4708(17)	0	0.3333(0)	1
P	0.4276(16)	0	0.8333(0)	1
O_1	0.4162(24)	0.3091(25)	0.3940(8)	1
O_2	0.4095(21)	0.2640(26)	0.8785(10)	1
R_{wp}		1.13%		
R_p		0.69%		
Cell parameters		a=5.0311Å		
		b=5.0311Å		
		c=11.2380Å		
Fe-O distance		Fe-O_1= 1.840(12)Å		
		Fe-O_2=1.790(8) Å		
		Fe-O(average)=1.815Å		

Formula		*$LiFePO_4$*		
Crystal system		*Orthorhombic*		
Space group		*Pnma*		
Atom	x	y	z	g
Li_1	0	0	0	1
Fe	0.28238(8)	0.25	0.97381(28)	1
P	0.09392(21)	0.25	0.4144(4)	1
O_1	0.0986(4)	0.25	0.7423(7)	1
O_2	0.4539(5)	0.25	0.2132(5)	1
O_3	0.16594(30)	0.0406(5)	0.2810(4)	1
R_{wp}		0.76%		
R_p		0.52%		
Cell parameters		a=10.3233Å		
		b=6.0053Å		
		c=4.6922Å		
Fe-O distance		Fe-O_1 = 2.187(4)Å		
		Fe-O_2 =2.097(4) Å		
		Fe-O_3 = 2.2590(23)Å		
		Fe-O_3 = 2.0370(28)Å		
		Fe-O(average) =2.145Å		

The XRD patterns and Rietveld refinement of the nano-$FePO_4$ (heat treatment at 600 ^oC for 10 h) and $LiFePO_4$/C nanocomposites are shown in Figure s3b and Figure s3c. The intense diffraction peaks indicate good crystallinity of both materials. Nano-$FePO_4$ is indexed well on the basis of trigonal $FePO_4$ with space group P3121, while $LiFePO_4$/C is indexed well on the basis of orthorhombic $LiFePO_4$ with space group *Pnma*. The observed and calculated patterns fit well to each other in Figure s3b and Figure s3c, which means that all elements are well located in their sites for both materials. Based on the calculated results of Rietveld refinement, the lattice constants and atomic parameters are listed in Table s1.

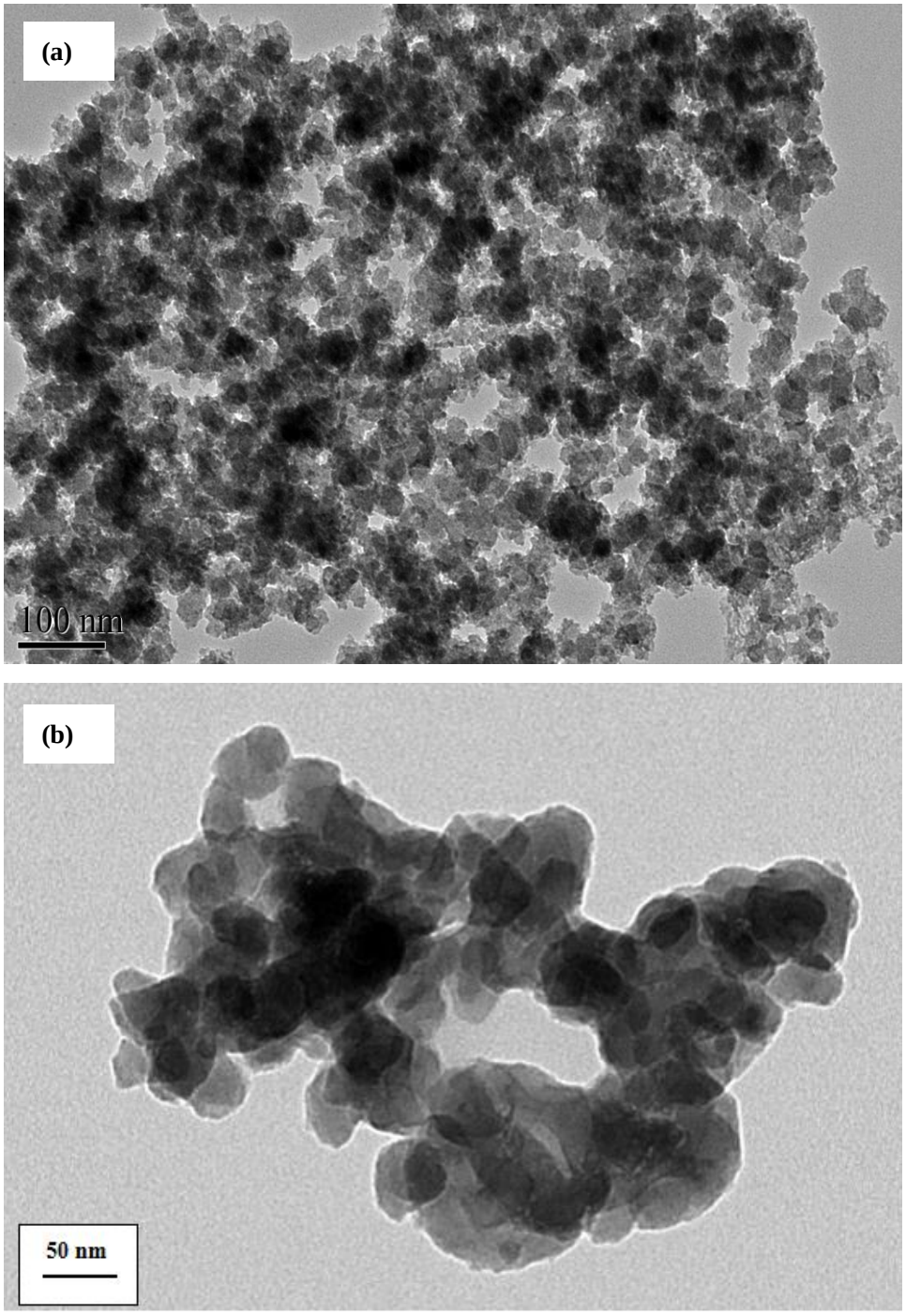

Figure s4. TEM of (a) precipitate; (b) precipitate calcined at 600 ℃ for 10 hours

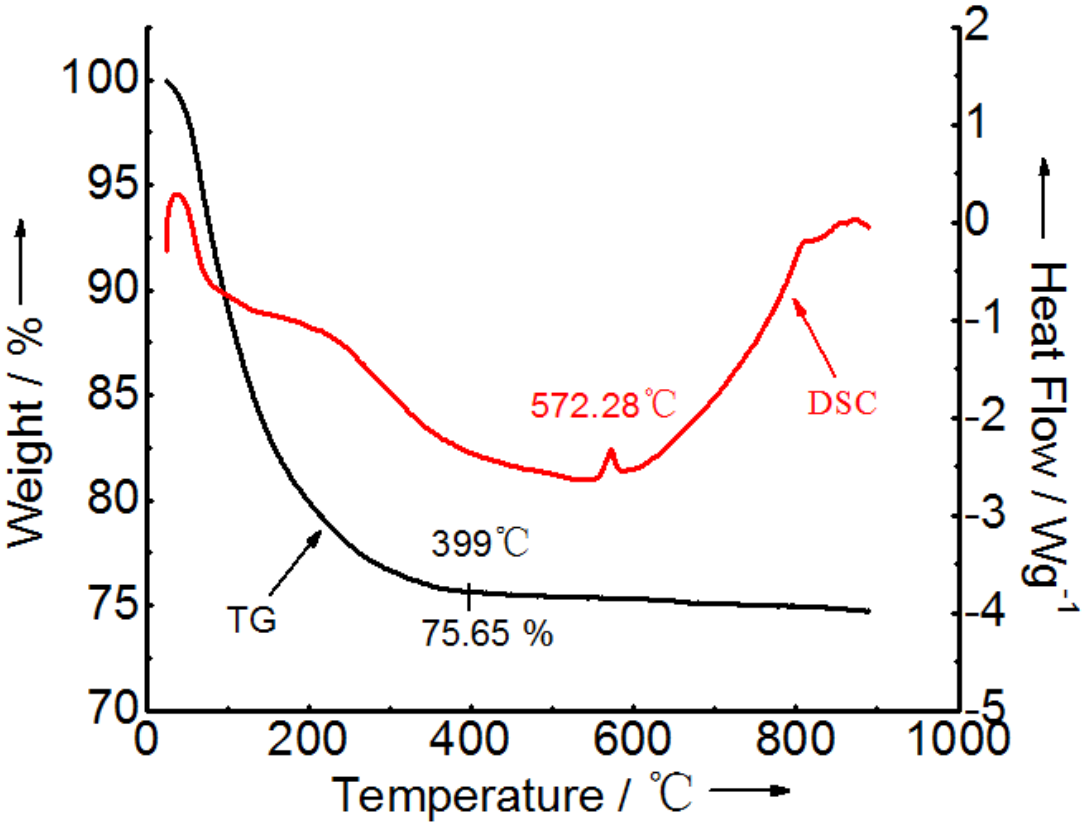

Figure s5. TG/DSC curves of the dried $FePO_4 \cdot xH_2O$

The x of $FePO_4.xH_2O$ is determined as 2.7 by TG analysis, which is in a good agreement with what reported by Kandori et al.[s1] The small exothermic peak detected at ~572 ^oC is attributed to the phase transition from the amorphous $FePO_4$ to the trigonal $FePO_4$.

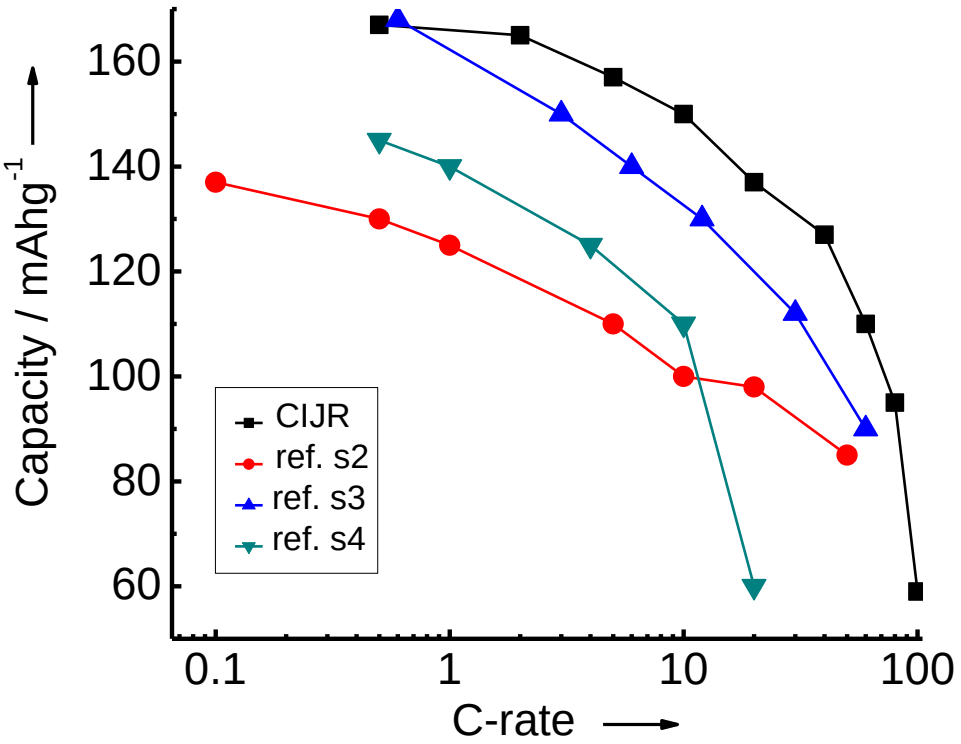

Figure s6. The rate capability of $LiFePO_4$/C prepared by CIJR compared with that from several earlier reports

Table s2. Detailed information of the $LiFePO_4$/C composite and the electrode

	The amount of carbon-coating	Particle size of primary particles	Weight ratio of $LiFePO_4$/C: Conductive Carbon:Binder	Loading of active material
CIJR	4.4 wt%	40-60 nm	75:15:10	4.2 $mg.cm^{-2}$
ref. 2	2 wt%	25 nm	80:10:10	3 $mg.cm^{-2}$
ref. 3	6 wt%	40-60 nm	83:12:5	5 $mg.cm^{-2}$
ref. 4	2 wt%	25 nm	90:6:4	N/A

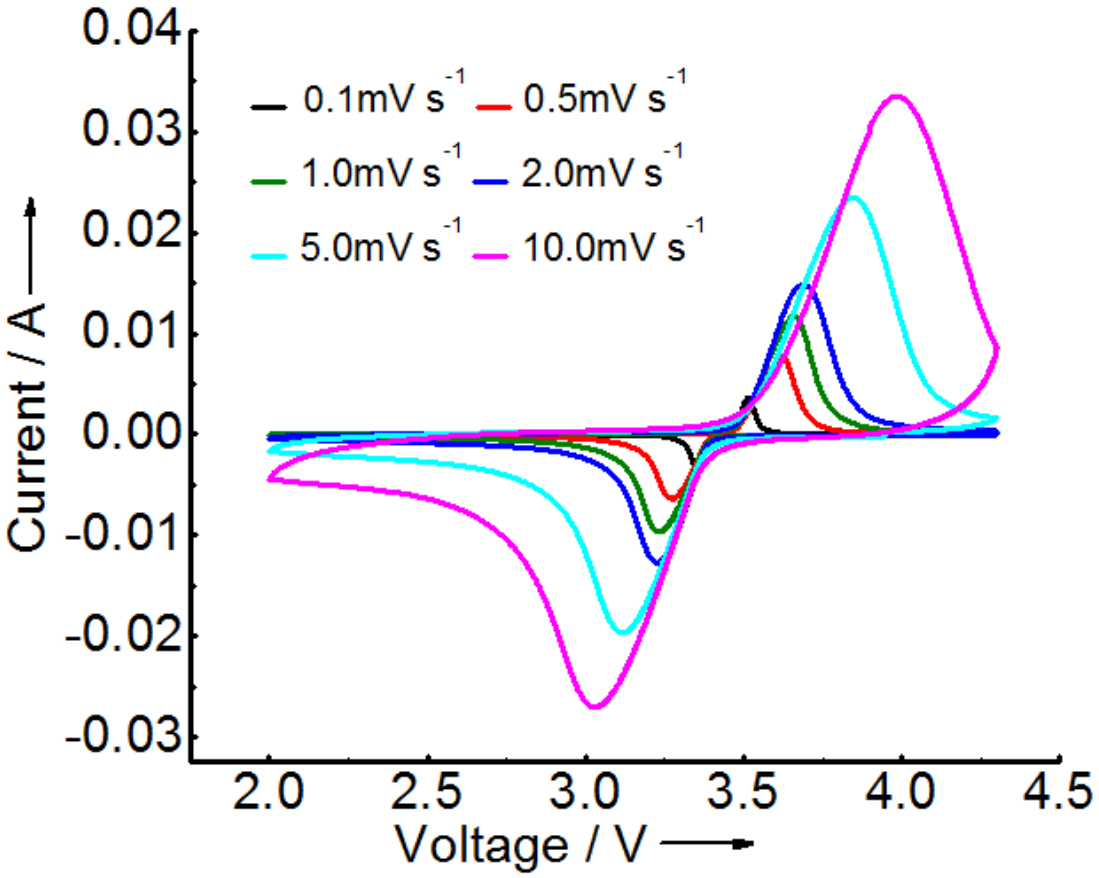

Figure s7. Cyclic voltammetry tests at different scan rates in the potential window 2.0-4.3 V (vs. Li^+/Li)

The cyclic voltammetry curve scanned at 0.1 mVs^{-1} reveals redox peaks centering at 3.52 V and 3.35 V vs. Li^+/Li, corresponding to Li^+ extraction and insertion processes, respectively. With the increase of the scan rate, the anodic peak shifts to high potential while the cathodic peak shifts to low potential, accompanied by the increase of the peak currents (i_p). The cathodic peak currents slightly lower than the anodic peak currents suggests the slightly kinetics difference between Li^+ insertion and extraction.

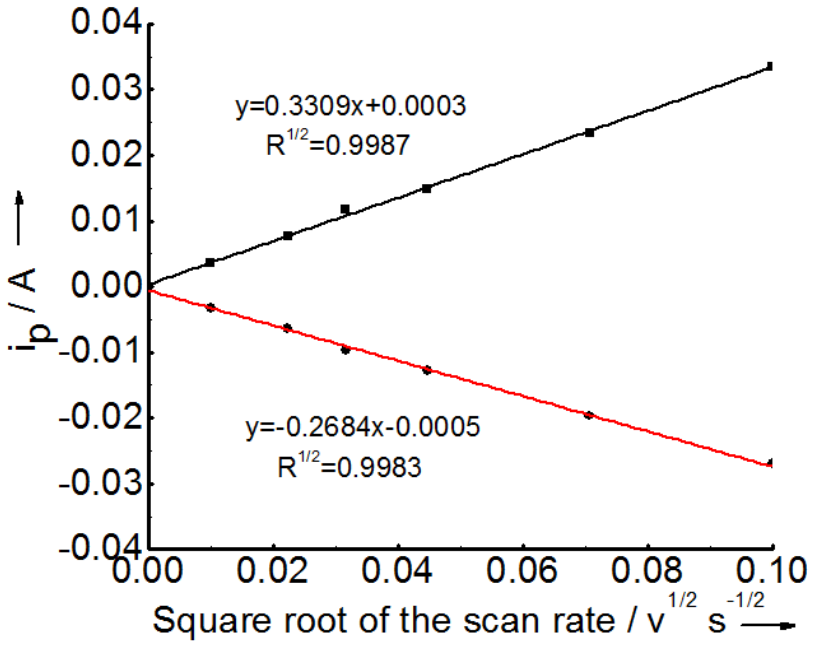

Figure s8. The half-order dependence of i_p on v

The half-order dependence of i_p on v suggests the reversible lithiation and delithiation processes are under semi-infinite diffusion control for the entire range of scan rates.[s5-s7] The diffusion coefficients calculated from the slope of i_p *vs* $v^{1/2}$ are 3.0×10^{-12} cm^2s^{-1} and 1.96×10^{-12} cm^2s^{-1} for delithiation and lithiation processes, respectively, which are within the reported range between 10^{-14} cm^2s^{-1} [s8] and 10^{-12} cm^2s^{-1} [s7,s8].

References:

s1 K. Kandori, T. Kuwae, T. Ishikawa, *J. Colloid and Interface Sc.*, 2006, **300**, 225.

s2 M.-H. Lee, J.-Y. Kim and H.-K. Song, *Chem. Commun.*, 2010, **46**, 6795.

s3 Y. Wang, Y. Wang, E. Hosono, K. Wang, and H. Zhou, *Angew. Chem. Int. Ed.*, 2008, **47**, 7461.

s4 K. Zaghiba, M. Dontignya, A. Guerfia, P. Charesta, I. Rodriguesa, A. Mauger, C.M. Julien, *J. Power Sources*, 2011, **196**, 3949.

s5 M. Takahashi, S. Tobishima, K. Takei, Y. Sakurai, *Solid State Ionics* 2002, **148**, 283.

s6 D. Yu, C. Fietzek, W. Weydanz, K. Donoue, T. Inoue, H. Kurokawa and S. Fujitani, *J. Electrochem. Soc.* 2007, **154**, A253.

s7 S. W. Song, Ronald P. Reade, Robert Kostecki, and Kathryn A. Striebel, *J. Electrochem. Soc.* 2006, **153**, A12.

s8 P. Prosini, M. Lisi, D. Zane, M. Pasquali, Solid State Ionics 2002, **148**, 45.